Electronic Supplementary Material (ESI) for Dalton Transactions.

Multifunctional MOFs through CO_2 fixation: a metamagnetic kagome lattice with uniaxial zero thermal expansion and reversible guest sorption

Tony D. Keene,[a,b] Michael J. Murphy,[b] Jason R. Price, [c,b] Natasha F. Sciortino,[b] Peter D. Southon[b] and Cameron J. Kepert.*[b]

[a] Chemistry, University of Southampton, University Road, Highfield, Southampton, SO17 1BJ, UK.
[b] School of Chemistry, The University of Sydney, NSW 2006, Australia.
[c] Australian Synchrotron Company Limited, 800 Blackburn Road, Clayton, Victoria 3168, Australia.
* cameron.kepert@sydney.edu.au

Table of contents

Characterisation of 1·H_2O

TGA: Compound **1**·H_2O undergoes three steps: the first is a loss of 1.4 % between 22 − 100 °C corresponds to loss of 1 × H_2O from $[Cu_3(CO_3)_2(bpac)_3](ClO_4)_2 \cdot H_2O$ (calculated 1.7%). The second is a sharp process centred at 283 °C with a mass loss of 51% and the third a broader process that continues to 600 °C. Inspection of the decomposition products revealed a mixture of Cu(II)O and Cu metal.

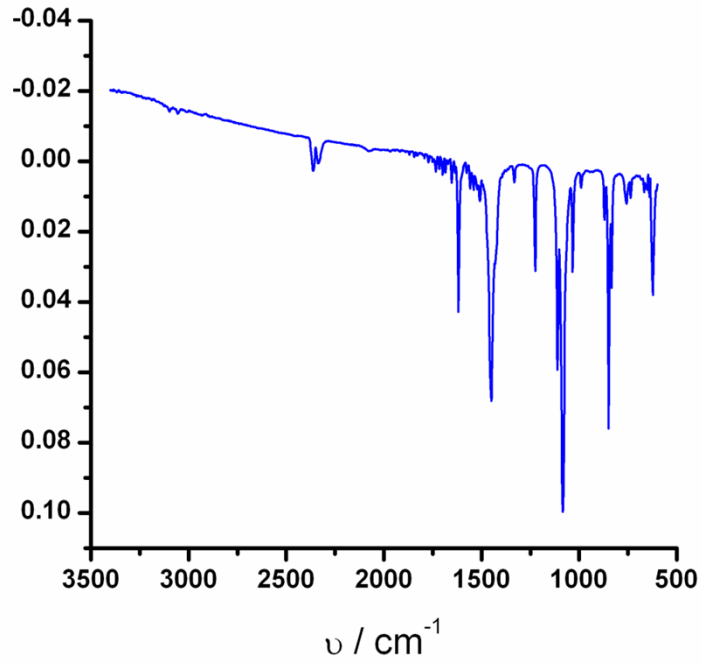

Figure S1 FTIR spectrum of **1**·H_2O.

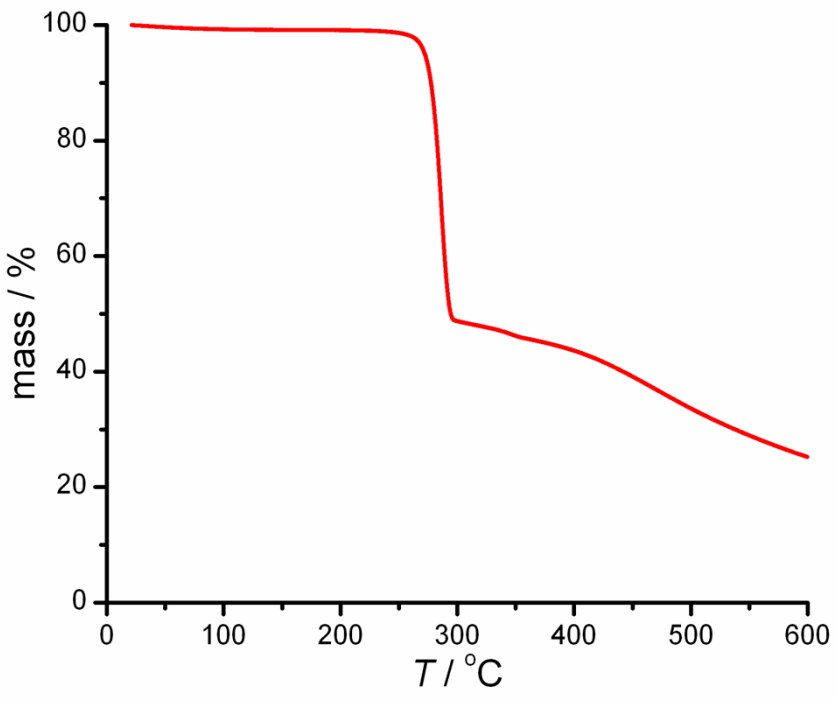

Figure S2 Thermogravimetric curve for **1**·H_2O in air.

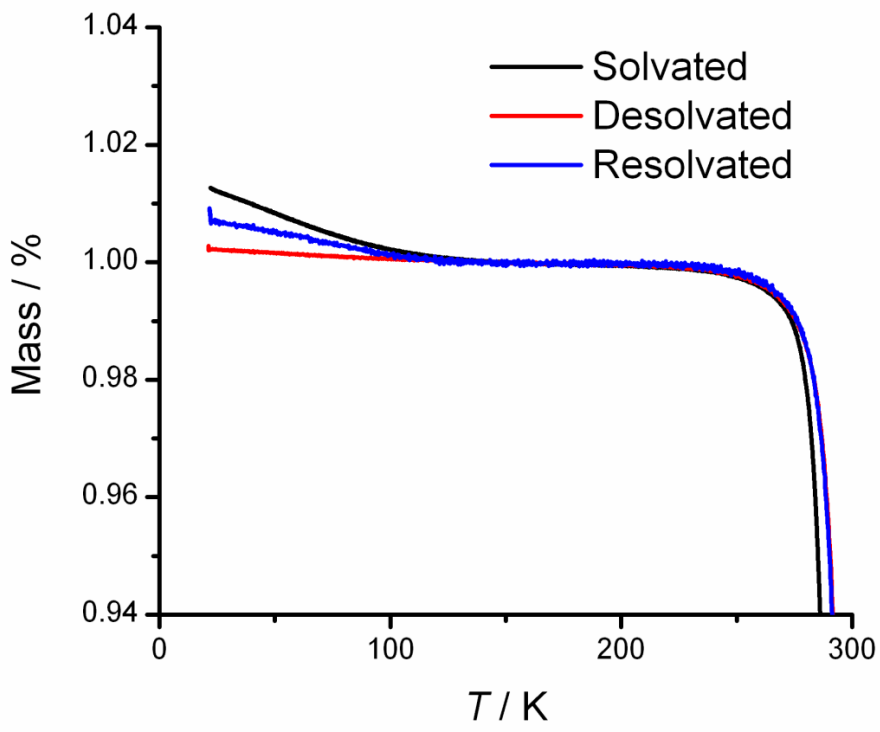

Figure S3 TGA of **1**·H_2O ('solvated', black), **1** ('desolvated', red) and resolvated **1**·H_2O (blue).

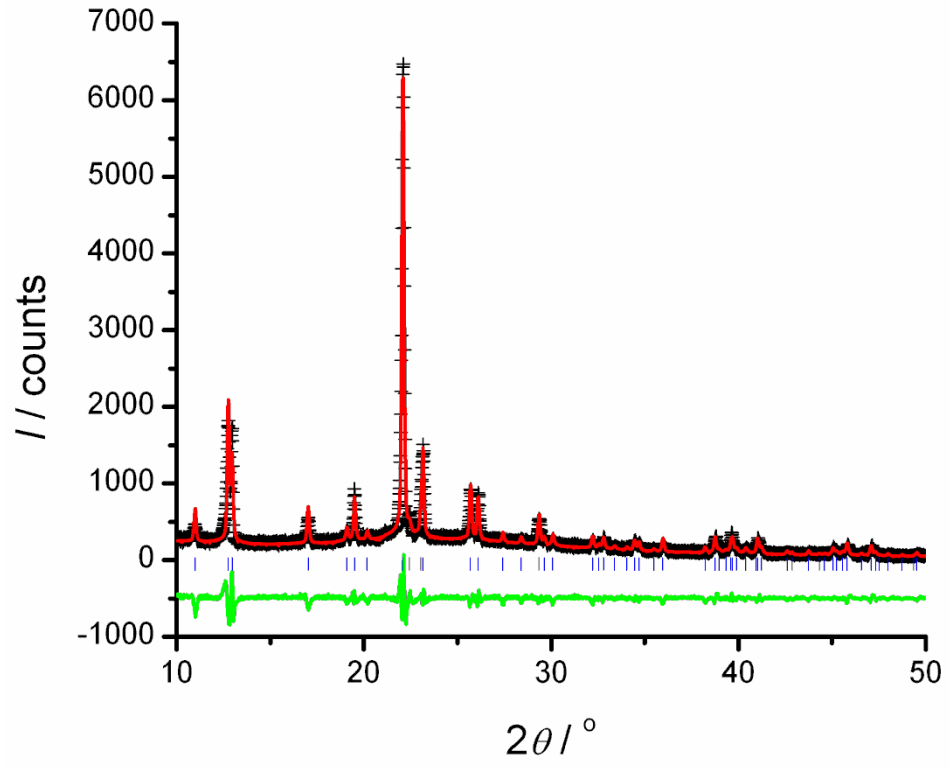

Figure S4 Powder X-ray diffraction plot for **1**·H_2O with Le Bail fit.

Crystal structure of 1·H_2O and 1

The asymmetric unit of **1**·H_2O consists of a Cu atom on ½, 0, ½ (Wyckoff site 3*g*), a bipyridylacetylene (bpac) along the ½, 0, *z* 2/*m* rotation axis with the centre of the C≡C bond on an inversion centre, a carbonate centred on ⅔, ⅓, ½ (6*k*), two perchlorate anions centred around 0, 0, 0 and 0, 0, 1/2 and a half-occupancy water molecule at centred around 0, 0, 0.26. The carbonate anion chelates three copper atoms through the $d_{x^2-y^2}$ (Cu−O = 1.955(3) Å) and d_{z^2} (Cu···O = 2.649(2) Å) orbitals to generate a $[Cu_3(CO_3)_2]_n^{2n+}$ kagome lattice in the *ab*-plane with Cu···Cu distances of 4.6000(1) Å. The layers are then pillared by the bpac ligands through the $d_{x^2-y^2}$ orbital with Cu−N bond distances of 2.001(4) Å and interlayer distances of 13.6033(3) Å. The kagome layers are stacked directly over each other to form hexagonal channels 8.185(6) Å wide at their narrowest in the *c*-axis. Within these channels lie the disordered perchlorates, one in the plane of the kagome layer, one in the plane of the acetylene groups of the ligands. Between the perchlorates, a disordered water molecule is found.
On desolvation, there are very small changes to the structure of the framework and the perchlorates remain disordered despite the removal of the water molecule between them. Below 150 K, there is a subtle structural modulation, which will be described in a further publication.

Table S1 Crystallographic parameters for **1**·H_2O and **1**

Formula	$C_{38}H_{26}Cl_2Cu_3N_6O_{15}$	$C_{38}H_{24}Cl_2Cu_3N_6O_{14}$
Formula mass / gcm^{-3}	1068.19	1050.18
Crystal system	Hexagonal	Hexagonal
Space group	*P*6/*m*	*P*6/*m*
a/Å	9.2000(2)	9.2577(3)
c/Å	13.6033(3)	13.5853(5)
V/Å^3	997.13(4)	1008.33(6)
ρ/g cm^{-3}	1.775	1.729
T/K	150(2)	350(2)
μ/mm^{-1}	1.800	1.777
Reflections collected	9572	5479
Unique reflections (R_{int})	692 (0.0224)	701 (0.0298)
Reflections I > 2σ(I)	672	582
Data/Restraints/Parameters	692/0/69	701/0/68
Goodness of fit (S)	1.259	1.053
*R*1/*wR*2 [F^2>2σ(F^2)]	0.0364/0.1090	0.0347/0.0988
*R*1/*wR*2 (all data)	0.0372/0.1096	0.0453/0.1071

Table S2 Significant distances (Å) and angles (°) for **1**·H_2O

Cu1−O1	1.955(4)	Cu1−O1*i*	2.649(2)	Cu1−N1	2.001(4)
C1−O1	1.282(2)	Cu1···Cu1*i*	4.6000(1)	O1−C1−O1*i*	120
O1−Cu1−N1	90	O1−Cu1−O1*i*	55.21(12)	O1−Cu1−O1*ii*	124.79(12)

Symmetry codes: *i*): 1−*y*, *x*−*y*, *z*; *ii*): *y*, −*x*+*y*, *z*.

Kagome HTSE model

To simulate a kagome lattice, the susceptibility of an n = 12, S = ½ ferromagnetically-coupled cluster with periodic boundary conditions was calculated using exact numerical full-matrix diagonalisation in OwPack (release 21/06/2006)[s1] using the following connectivity map with g = 2 and J/k_B = 1 K:

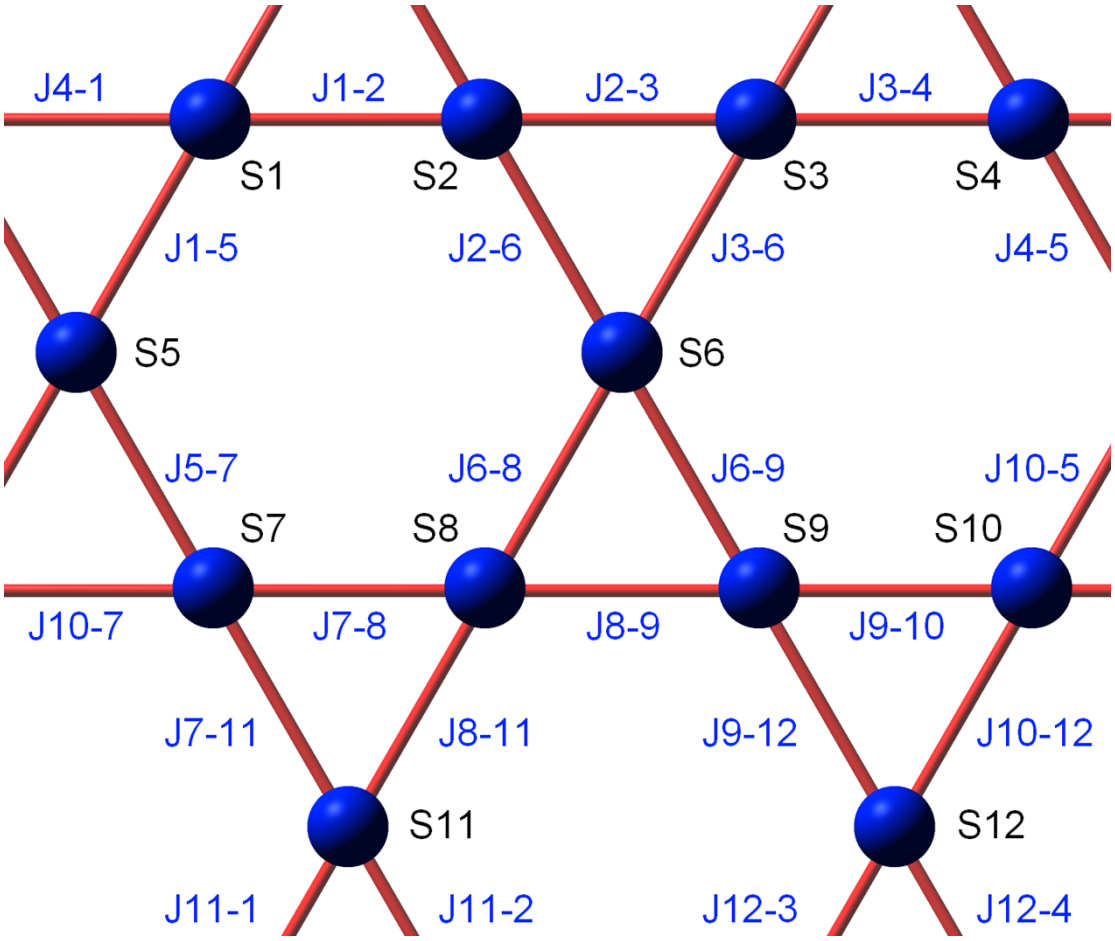

Figure S5 Connectivity map for an n = 12 cluster with periodic boundary conditions used for simulating a ferromagnetic kagome lattice.

From our previous work into ferromagnetic layers,[s2] we expect that this model will be accurate at temperatures above 1.2 × J/k_B. We then modelled this simulation in the valid region by varying eight parameters in a series for n = 8:

$$H = -J\sum_{ij} S_i \cdot S_j \qquad \text{eq. S1}$$

$$\chi = \frac{Ng^2\mu_B^2}{3k_BT} \cdot S(S+1) \cdot \left(1 + \sum_{n=1}^{n=8} a_n (J/k_BT)^n\right) \qquad \text{eq. S2}$$

Eight parameters gave an excellent fit to the simulation with $\chi^2 = 5.49 \times 10^{-15}$. Fitting the simulation with the refined *a* parameters in equation 2 in the same temperature range returned a *g*-value of 2 with an error of 5.74×10^{-8} and a coupling of 1.000005 with an error of 1.14×10^{-7}, far below the usual experimental error of magnetic susceptibility measurements (ca. 0.1-1% due to sample weighing accuracy and diamagnetic correction).

n	**value**	***n***	**value**
1	1	5	−0.00464
2	0.5	6	−0.01962
3	0.06262	7	−0.04166
4	−0.03765	8	0.02789

Table S3 a_n parameters for $S = ½$ ferromagnetic kagome lattice HTSE.

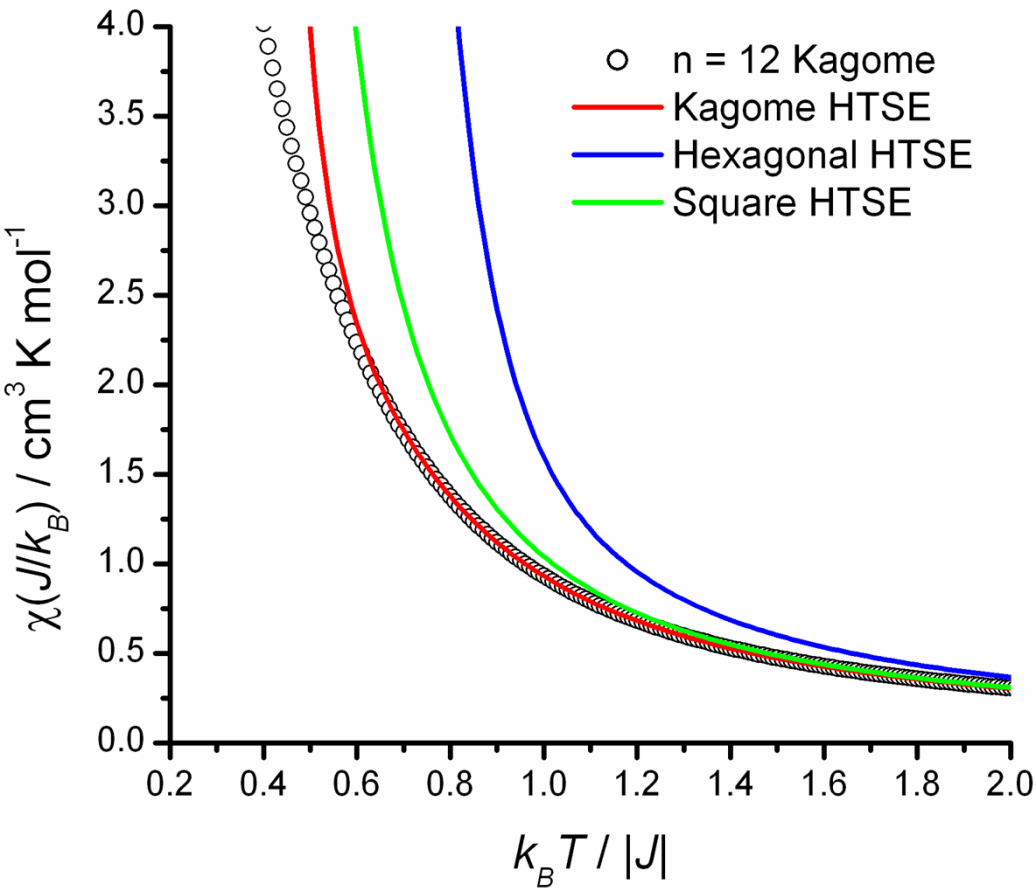

Figure S6 Reduced susceptibility plot of $S = ½$, $n = 12$ kagome simulation, our $S = ½$ kagome HTSE, Rushbrooke *et al.*'s $S = ½$ hexagonal lattice HTSE and Oitmaa and Bornilla's $S = ½$ quadratic HTSE.

Use of equation 2 may present some difficulty in estimating the temperature range in which to model the susceptibility of a new compound due to the $k_BT/|J|$ range in which the equation is valid being higher in temperature than the sharp increase in susceptibility.

As such, inspection of the Weiss constant derived from the calculated data shows the relationship $J/k_B = 1.064 \times \theta$, therefore $T_{\min} = 1.277 \times \theta$. Normally, this would give an excellent starting point from which to estimate the coupling constant and temperature range over which the model is valid, but Weiss constants are affected by interlayer coupling and small discrepancies in diamagnetic correction. The most effective approach is to model the high-temperature data, obtain an initial estimate of the coupling and measure over a range derived from that coupling.

Comparison of other models for ferromagnetic layers is of interest here: plotting the reduced susceptibility of the $S = ½$ $n = 12$ kagome simulation, our $S = ½$ kagome HTSE, Rushbrooke *et al.*'s $S = ½$ hexagonal HTSE[s3] and Oitmaa and Bornilla's $S = ½$ quadratic HTSE,[s4] we find that despite the Kagome layer being a derivative of the hexagonal layer, the closest model is in fact the quadratic. This is due to the connectivity of the layers – in the hexagonal model, there are six couplings to neighbouring $S = ½$ centres, while in the kagome and quadratic models, each centre is four-connected. The hexagonal model significantly underestimates the coupling in a kagome lattice.

Magnetism

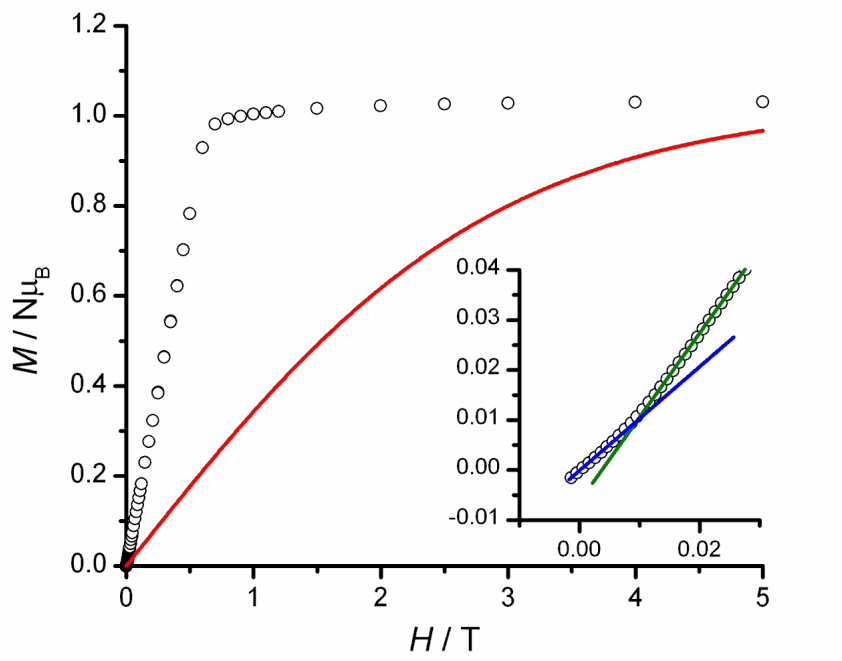

Figure S7 Magnetisation plot of **1**.H_2O at 2 K with Brillouin curve for g = 2.100. Inset: inflection at 0.01 T, marking the metamagnetic transition field (lines shown as guides to the eye).

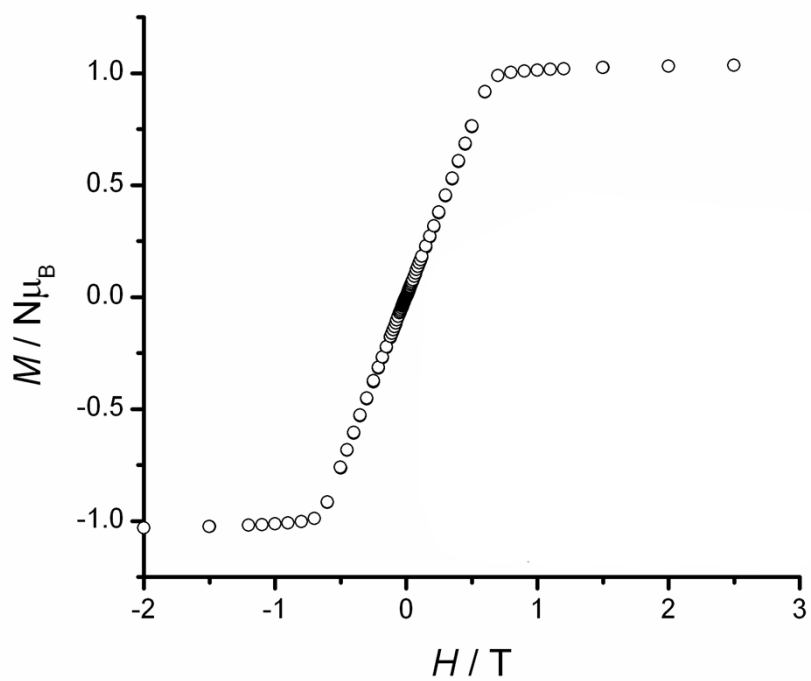

Figure S8 Magnetisation loop for **1**·H_2O at 2 K showing lack of magnetic hysteresis.

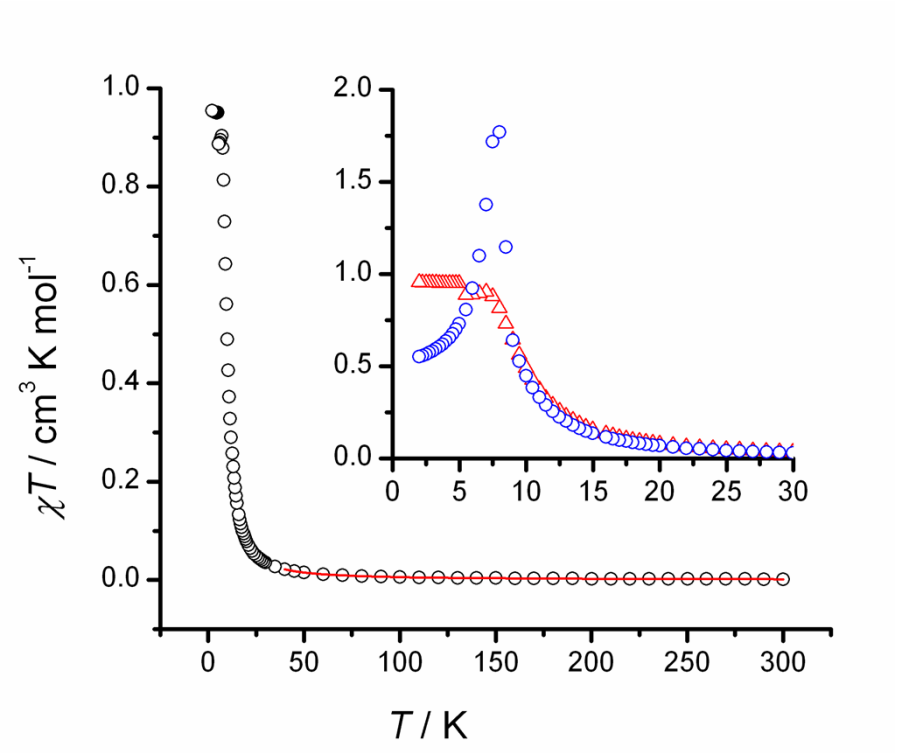

Figure S9 Magnetic susceptibility of **1** at 0.2 T with fit from S = ½ ferromagnetic kagome polynomial (solid red line) with g = 2.161(3) and J/k_B = +28.3(3) K. Inset: magnetic susceptibility at 0.004 T (○) and 0.2 T (Δ).

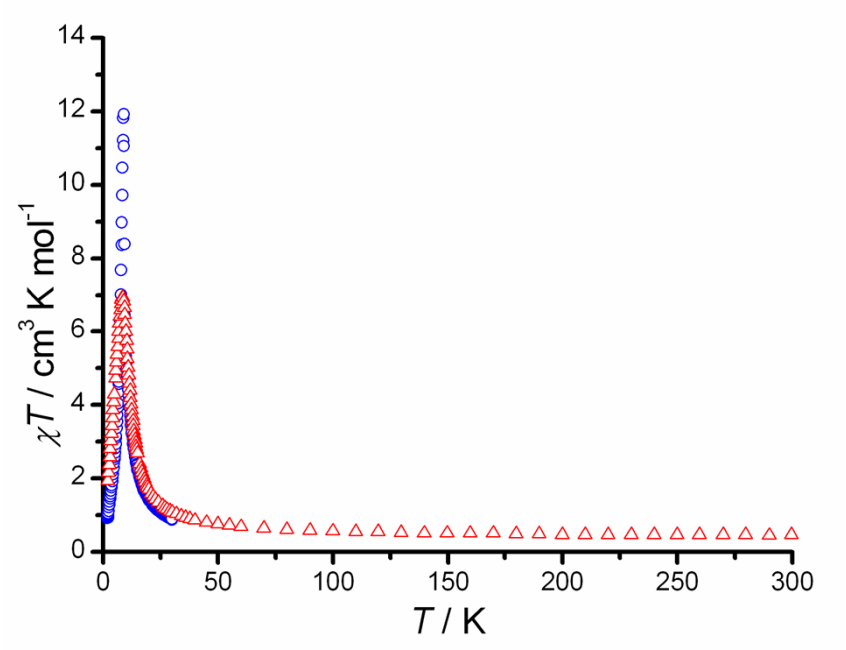

Figure S10 $\chi T(T)$ plot for **1**·H_2O at 0.004 T (○) and 0.2 T (Δ).

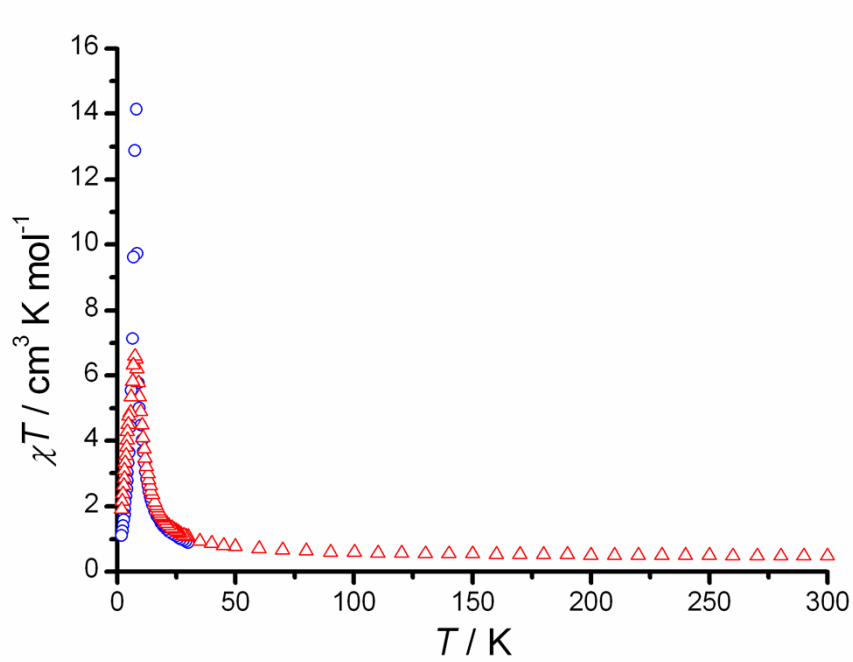

Figure S11 $\chi T(T)$ plot for **1** at 0.004 T (○) and 0.2 T (Δ).

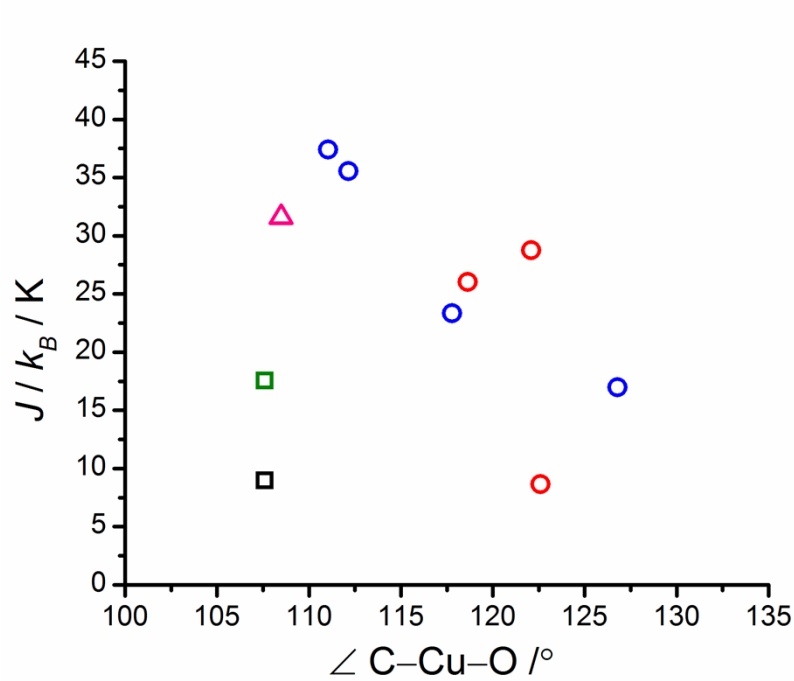

Figure S12 Plot of C−O−Cu angle *vs* magnetic coupling. Data shown: trigonally-symmetric $Cu_3(CO_3)$ trimeric species (○); data from nearly-symmetric trimers (○); data from ref. S9 hexagonal model (□) and kagome model (□); data from this work for **1**·H_2O (Δ).

In Figure S12, a roughly linear relationship can be seen between C–O–Cu angle and coupling strength when considering the trigonally-symmetric data (○) and less-symmetric

compounds (○) with averaged angles where the range in angle is less than 10% of the average. The reported couplings fit very well with the predicted values by Félix *et al.* (see figure 8 in that paper – in a trigonally-symmetic case, C–O–Cu angles convert to their system as follows $\alpha_1 = 360° - (\angle C–O–Cu + 30°)$ and $\alpha_1 = \angle C–O–Cu - 30°$.

CSD code	**Cu−O / Å**	**C−O−Cu / °**	**α_1 / °**	**α_2 / °**	**J/k_B / K**		**ref**
IFIDOR	1.976	117.78	212.22	87.78	16.23	○	[S5]
NOJZOB	2.001	112.14	217.86	82.14	24.7	○	[S6]
RAMVIL	1.972	111.05	218.95	81.05	26	○	[S7]
ZINXAV10	1.933	126.78	203.22	96.78	11.8	○	[S8]
ZOKDIM	1.971	118.64	211.36	88.64	18.1	○	[S9]
IBOLAO	1.906	122.59	207.41	92.59	6	○	[S10]
OGEHIR	1.988	122.1	207.9	92.1	19.99	○	[S11]
WANLED	1.951	107.6	222.4	77.6	12.2 (k) 8.96 (h)	□ □	[S12]
This work	1.955	108.48	221.52	78.48	31.5	Δ	-

Table S4 Structural parameters and coupling constants of $[Cu_3(CO_3)]$ complexes. 'k' refers to the coupling obtained by the $S = ½$ ferromagnetic kagome model and 'h' to the $S = ½$ hexagonal model.

References

[S1] O. Waldmann, *Phys. Rev. B*, 2000, **61**, 6138-6144; O. Waldmann, H. U. Güdel, T. L. Kelly and L. K. Thompson, *Inorg. Chem.*, 2006, **45**, 3295-3300.

[S2] T. D. Keene, Y.-H. Deng, F.-G. Li, Y.-F. Ding, B. Wu, S.-X. Liu, C. Ambrus, O. Waldmann, S. Decurtins and X.-J. Yang, *Inorg. Chim. Acta*, 2009, **362**, 2265-2269.

[S3] G. S. Rushbrooke, G. A. Baker and P. J. Woods in *Phase Transitions and Critical Phenomena, vol. III* (Eds.: C. Domb, M. S. Green), Academic Press, New York, 1975, ch. 5.

[S4] J. Oitmaa and E. Bornilla, *Phys. Rev. B*, 1996, **53**, 14228-14235.

[S5] D. Hu, L. Chen, Z.-Q. Pan, H. Liu, X.-G. Meng and Y. Song, *J. Coord. Chem.*, 2008, **61**, 1973-1982.

[S6] J. Springborg, J. Glerup and I. Søtofte, *Acta Chem. Scand.*, 1997, **51**, 832-838.

[S7] J. Mukherjee, R. Gupta, T. Mallah and R. Mukherjee, *Inorg. Chim. Acta.*, 2005, **358**, 2711-2717

[S8] C. Bazzicalupi, A. Bencini, A. Bencini, A. Bianchi, F. Corana, V. Fusi, C. Giorgi, P. Paoli, P. Paoletti, B. Valtancoli and C. Zanchini, *Inorg. Chem.*, 1996, **35**, 5540-5548.

[S9] A. Escuer, R. Vicente, E. Peñalba, X. Solans and M. Font-Bardía, *Inorg. Chem.*, 1996, **35**, 248-251.

[S10] P. Mateus, R. Delgado, F. Lloret, J. Cano, P. Brandão and V, Félix, *Chem. Eur. J.*, 2011, **17**, 11193-11203.

[S11] M. Rodríguez, A. Llobet, M. Corbella, P. Müller, M. A. Usón, A. E. Martell and J. Reibenspies, *J. Chem. Soc. Dalton Trans.*, 2002, 2900-2906.

[S12] A. Majumder, C. R. Choudhury, S. Mitra, G. M. Rosair, M. S. El Fallah and J. Ribas, *Chem. Commun.*, 2005, 2158-2160.